Available online at www.sciencedirect.com
SCIENCE DIRECT
Polymer 45 (2004) 4307–4314
polymer
www.elsevier.com/locate/polymer

Static and dynamic studies of phase composition in a polydisperse system

Ian Hopkinson[a,*], Matthew Myatt[b], Ali Tajbakhsh[b]

[a]Department of Physics, UMIST, Sackville street, P.O. Box 88, Manchester M60 1QD, UK
[b]Cavendish Laboratory, University of Cambridge, Madingley Road, Cambridge CB3 0HE, UK

Received 16 October 2003; received in revised form 29 March 2004; accepted 5 April 2004

Abstract

We have conducted a study of the phase compositions of a ternary solution containing dextran/polyethylene glycol (PEG)/water using UV–visible spectrometry to study the equilibrium behaviour and confocal microscopy to study the dynamic behaviour observed when the system undergoes phase separation driven by the loss of water. Such a study of phase compositions using confocal microscopy is a new development of the technique. In the static experiments, we find a cloud curve, which lies above the coexistence curve on the PEG rich side of the phase diagram, this is found to be in qualitative agreement with calculations of the phase behaviour for a model polydisperse system. In the dynamic experiments, we are able to measure the phase composition using confocal microscopy in the late stages of separation. Here, the compositions lie well inside the coexistence curve at lower drying rates but converge with it at higher drying rates. This is linked to a change in phase morphology: at low rates, a droplet morphology is observed throughout the process whilst at high drying rates a gross phase separation into two layers is observed to occur even at the earliest times probed by the experiment.

Keywords: Polymer physics; Polymer physical chemistry; Ternary solution

1. Introduction

Phase separation is a phenomenon which is common in industrial processes and as such has received much academic attention. For polymeric systems, it has long been recognised that the presence of polydispersity, either in the molecular weight of species or in their composition, leads to added complexity in phase behaviour. Polymeric systems are experimentally amenable because the large size of the species means that time scales for macroscopic phase separation are relatively long and length scales of phase separated phases are relatively large when compared to other molecular systems.

Studies of phase separation in polymer systems have focussed on the developing morphology observed when a system is 'homogeneously' quenched from the one phase region to the two phase region. This quench is normally achieved by imposing a step change in temperature upon the system. Following this step change, the temperature is fixed and the subsequent evolution of the two phase morphology is observed, often using light scattering [1–4], but more recently using confocal microscopy [5–10]. The evolution of morphology is understood in terms of the Cahn–Hilliard model [11–13] for critical quenches at short times and Binder–Stauffer [14], Lifshitz [15] and Siggia [16] theories of phase coarsening at later times.

Experiments on systems subjected to a step quench are important in understanding many aspects of phase separation, however, in practical applications quenches are often non-uniform and may not occur very rapidly. In this work, we study a 'solvent' quench; a ternary polymer solution (dextran–polyethylene glycol (PEG)–water) in the one phase region which is driven to phase separation by allowing the water to evaporate from the sample. This evaporation is allowed to proceed throughout the experiment and so the quench is 'continuing', meaning that the equilibrium compositions of the coexisting phases change with time. We follow the development of the phase-separated system using confocal microscopy. This type of solvent quench is important in processes such as spin-coating, film-casting, spray drying and freeze drying.

In previous work [17] we have shown how laser scanning

* Corresponding author. Tel.: +44-161-306-8881; fax: +44-161-200-3941.
E-mail address: i.hopkinson@umist.ac.uk (I. Hopkinson).

0032-3861/$ - see front matter © 2004 Elsevier Ltd. All rights reserved.
doi:10.1016/j.polymer.2004.04.006

confocal microscopy (LSCM) can be used to probe the morphology as phase separation proceeds, in this system the complexity is increased because gravity also plays a part, since the phase separated phases have different densities. In this work, we will focus on the development of the phase compositions during the quench. To our knowledge, such a study is unique, although very recently Maeda et al. [18] demonstrated the use of confocal Raman microscopy to measure phase compositions at equilibrium. This type of study, where the phase composition is investigated, is not appropriate to systems which have been subjected to a step quench since the phase compositions in such a system rapidly reach equilibrium and subsequent development is only in the morphology of the phases.

LSCM [19–21] is a development of conventional optical microscopy whereby only light from the focal plane of the microscope is detected. This makes it straightforward to acquire 3D images of a translucent sample by taking a succession of 2D images and moving the sample between each image. Contrast in confocal microscopy is typically achieved by the use of fluorescent dyes, a technique which is heavily utilised in the biological sciences. In the physical sciences particularly notable are the studies of colloidal materials by van Blaaderen et al. [22,23] and Weeks et al. [24,25] and phase separated morphology in polymer systems by Ribbe et al. [5,6], Jinnai et al. [7–9] and Takeno et al. [10]. In these experiments, fluorescence labelling has been key because refractive index contrast is difficult to engineer. Furthermore, techniques such as differential interference contrast and phase contrast that are often used in materials science studies are difficult to achieve in LSCM due, in part, to the thickness of the sample and the complexity of the necessary optics.

Previous studies of dried films of ternary polymer solutions by Kumacheva [26], Mitov [27], Serrano et al. [28] and Müller-Buschbaum [29] have focussed on the final morphology of a dried layer. Kumacheva and Mitov, studying films formed by the evaporation of polystyrene/poly(methyl methacrylate)/toluene, found regular arrays of droplets of one phase at the air–film interface above a layer depleted in that phase. They attributed this behaviour to Benard–Marangoni convection. Müller–Buschbaum, on the other hand, concentrated on the surface topology of films prepared by the drying of polystyrene/polybromostyrene/solvent solutions using a wide range of solvents to study their effect on the final morphology.

The dextran–PEG–water system is widely used in the biotechnology industry to separate biological molecules. It [30–33], and its components [34,35] have been the subject of numerous detailed thermodynamic studies and it has been recognised that polydispersity in the dextran produces significant effects in the phase behaviour of this system [36].

2. Experimental methods

2.1. Materials

The dextran used in this study was purchased from Sigma (catalogue number D4876, lot number 79H0170) and is quoted as having average $M_w = 148,000$. The molecular weight distribution is approximately Gaussian in shape and is very wide, having a polydispersity ratio of around 2.8 [36] (corresponding to a standard deviation of $\pm 67{,}000$ Da).

Dextran was labelled by the addition of 1.0 wt% of dextran–fluorescein isothiocyanate (dextran–FITC), a covalent complex between dextran and the common fluorescent label fluorescein, which was supplied by Fluka (catalogue number 46946, $M_w = 150,000$). The degree of labelling of the dextran–FITC is quoted by the manufacturer as corresponds to approximately six fluorescein labels per dextran molecule.

The PEG used in this work was purchased from Sigma (catalogue number P4463, lot number 69H00342). The average M_w is quoted as 8000 and the distribution is likely to lie within the range 7000 and 9000 [37]. We synthesised a covalently bonded rhodamine–PEG complex, which was added at a level of 0.1 wt%, to serve as a label for the PEG. Details of the synthesis and characterisation of the labelled PEG can be found in Ref. [38]. Each PEG molecule was labelled with an average 1.39 rhodamine molecules.

2.2. Methods

Prior to the microscopic study of phase separation, the phase diagram of the dextran–PEG–water systems used here were determined using UV–visible absorption spectroscopy; in addition the cloud point curve was determined. Experiments were all conducted in phosphate buffered solutions (pH = 7.65), since the fluorescence behaviour of fluorescein is strongly affected by pH [39].

UV–visible spectra were acquired using a Unicam UV/visible spectrometer; samples were all measured in the same quartz cuvette with 10 mm path length. To determine the coexistence curve for the system, solutions of different overall polymer content but fixed ratios of PEG and dextran were prepared and allowed to phase separate over a period of at least 48 h. Total polymer concentrations were in the range of 83–90 wt%; the dextran:PEG ratio was chosen such that the volume fraction of dextran rich phase in the separated system is $\phi_{dex} = 0.5$.

After the two phases had separated they were carefully extracted using a syringe and diluted 1:5 (v/v) before UV–visible spectra were acquired. This dilution ensures that no further phase separation occurs and that there are no non-linear effects or saturation in the UV–visible spectra. Phase compositions for dextran and PEG were determined in separate experiments, i.e. in one set of experiments, labelled dextran and unlabelled PEG were used whilst in a second set unlabelled dextran and labelled PEG were used. This

procedure allows the most accurate determination of phase compositions, furthermore it matches exactly the procedure which must be used in the acquisition of the confocal images.

The cloud point curve was determined for mixtures of dextran and PEG solutions with dextran:PEG mass ratios in the range 1:9 to 9:1.

Following these determinations of the bulk phase diagram, microscopic investigations of single component films and films of ternary solutions undergoing phase separation by drying were carried out. Ternary solutions were prepared with a PEG:dextran ratio such that the phase separated system had a volume ratio $\phi_{dex} = 0.34$. The overall polymer concentration was initially fixed such that the solutions were slightly above the cloud point curve—in the one phase region of the phase diagram.

A fixed volume of solution was injected into a 30 mm diameter polystyrene Petri dish to give a film with an initial thickness of 245 ± 15 μm. The sample was placed onto the stage of a Zeiss LSM510 upright confocal microscope ready for observation with a ×20 dry objective lens (NA = 0.5). The sample and objective lens were surrounded with a polycarbonate enclosure through which dry nitrogen was passed at a known flow rate. The drying rate was varied by altering the flow rate of the nitrogen. A pipe heater was used to keep the temperature of the nitrogen at 22 ± 1 °C. The microscope stage was carefully levelled such that the base of the petri dish was horizontal. The meniscus formed by the liquid at the sides of the dish extends for only a couple of millimetres so that the liquid surface was flat across most of the petri dish. The drying rate, Γ, was used as a parameter in these experiments.

The FITC–dextran was imaged by laser excitation at 488 nm and detection of fluoresced light with wavelengths longer than 505 nm. The rhodamine–PEG was imaged by laser excitation at 543 nm and detection of fluoresced light with wavelengths longer than 560 nm. Although it is possible to image FITC–dextran and rhodamine–PEG simultaneously resonant energy transfer (RET) (whereby the FITC is excited but transfers energy, by interaction, to the rhodamine which then fluoresces) means that quantitative analysis of the fluorescence intensity to obtain composition becomes impossible [40]. For this reason, experiments on ternary solutions were conducted in pairs in the first experiment of the pair only the dextran was fluorescently labelled whilst in the second experiment only the PEG was labelled. This mirrors the procedure used to determine the bulk phase diagram.

3D image stacks covering the entire depth of the film were acquired at intervals of 1 min or more for the drying experiments. Each image stack consisted of 30 horizontal slices with 256 × 256 pixels and covering an area of 230 μm × 230 μm. The vertical spacing of the image slices was gradually reduced during the experiment as the sample became thinner due to water loss, typically ranging between 11 and 6 μm. The nominal thickness of the focal plane is approximately 5.3 μm. The laser intensity, scan speed and pixel averaging were carefully chosen to obtain the best compromise between image stack size, acquisition time, image noise and sample bleaching. Typically, the first acquisition commenced ~2 min after the solution was placed in the petri dish. Images were acquired at 1 min intervals for periods between 10 min for the fastest drying solutions and 35 min for the slowest drying solutions.

3. Results and discussion

Fig. 1 shows the bulk phase diagram for our dextran/PEG/water system determined from a mixture with $\phi_{dex} = 0.5$, also included are data from the literature by Diamond and Hsu for mixtures of similar molecular weight [30]—there is good agreement between the two sets of data. This shows that the incorporation of a fluorescent dye does not lead to gross changes in the phase diagram in this instance. Fig. 1 also shows the cloud point curve. For higher dextran concentration the cloud point curve and the coexistence curve coincide, whilst at lower concentrations they do not. This is a consequence of the relatively large polydispersity of the dextran phase, which we will discuss in more detail below. We observe very similar coexistence curves for $\phi_{dex} = 0.66$ and 0.34.

The observed cloud point behaviour is not the result of phase separation of pure PEG solutions—we have found that the PEG used in this work is soluble to at least 20 wt%, which is consistent with other works in the literature [33,34].

The effect of polydispersity on phase behaviour has long been recognised, its effect on the behaviour of a single polydisperse polymer dissolved in a solvent were first considered by Koningsveld and Staverman [41,42]. Since then there has been considerable development in the theoretical methods used to calculate phase behaviour in

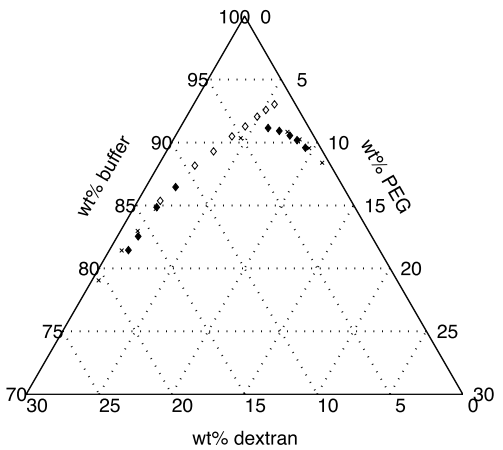

Fig. 1. Phase diagram for the dextran/PEG/buffer system in weight percentage. (◇) cloud point curve, (◆) coexistence curve measured for $\phi_{dex} = 0.5$ and (×) coexistence curve measured by Diamond and Hsu [30].

such systems. These are summarised by Sollich [43]. Its relevance to the phase behaviour of the PEG–dextran–water system has already been highlighted by Kang et al. [36].

Here, we will simply show the results of some basic calculations based on the method described by Solc [44]. We consider a mixture of two components A and B. Component A represents dextran and is comprised of three fractions with degree of polymerisation $N = 500$, 1000 and 1500 in the ratio 0.25:0.5:0.25. Component B represents the dextran phase and contains fractions with $N = 80$, 100 and 120 in the ratio 0.25:0.5:0.25. These components are selected to represent the relative degrees of polymerisation of the dextran and PEG components and their relative polydispersities. Coexistence curves and cloud point curves are calculated for this system and are shown in Fig. 2. This phase diagram is calculated in the polymer composition/temperature plane (the interaction parameter g is inversely proportional to temperature and so plotting the data against $-g$ produces a graph with the same shape as a plot against temperature). It will have qualitatively the same behaviour as the phase diagram in which we are interested, which lies in the polymer composition/solvent plane.

We see from Fig. 2 that the critical point is shifted towards the PEG rich side of the phase diagram and that the cloud point curve is close to the coexistence curve on the dextran rich side of the critical point but moves away from it on the PEG rich side. These results are consistent with our experimental observations.

As a prelude to looking at phase separating solutions, measurements on layers of the pure components were made. These showed that there was some surface enrichment of PEG, as might be expected [45] and that the effect of optical absorption through the film was small enough to be ignored in subsequent data analysis.

In our earlier work [17], we discussed the development of

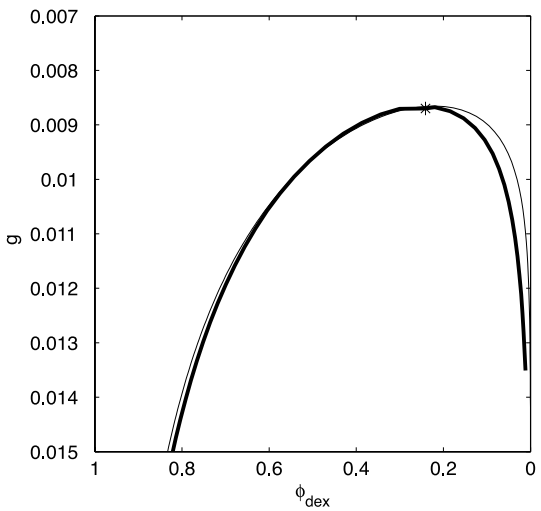

Fig. 2. Calculated phase diagram for a model dextran–PEG–water system, the thick line represents the coexistence curve and the thin line the cloud point curve. The critical point is indicated by $*$.

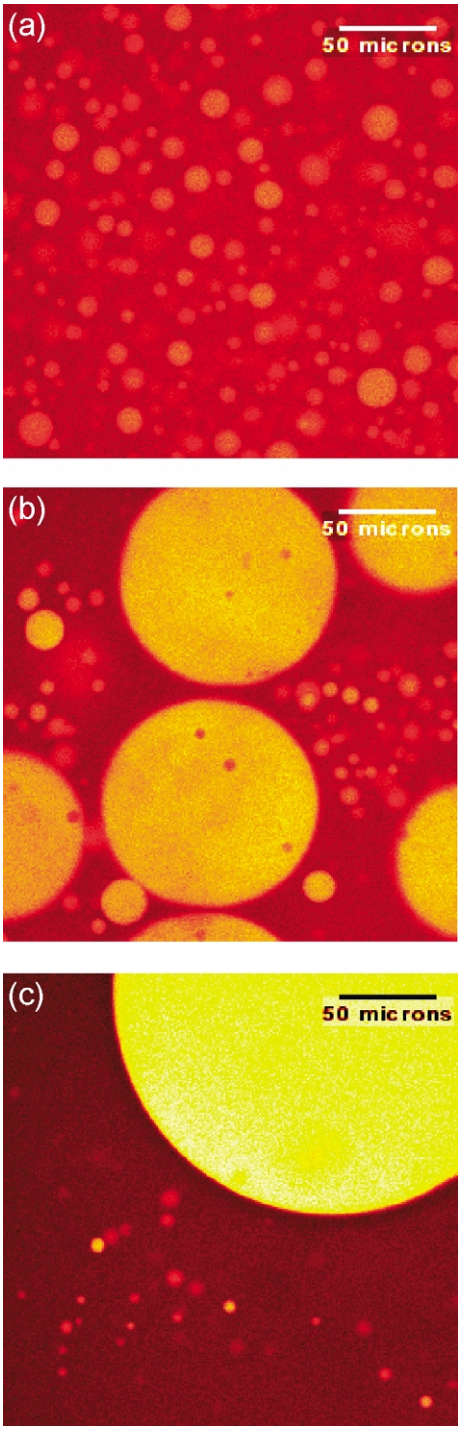

Fig. 3. Confocal images from near the bottom of a phase separating dextran labelled system illustrating a clear change in contrast and hence composition with time. Drying rate, $\Gamma = 6.55 \times 10^{-5}$ kg m^{-2} s^{-1}. Overall buffer content (a) 89.5 wt%, (b) 88.6 wt% and (c) 85.9 wt%.

phase morphologies in some detail. To summarise briefly on drying ternary solutions with $\phi_{dex} = 0.34$, phase separation is observed to occur first of all as a layer of droplets near to the upper surface of the sample. These droplets, being denser than the continuous phase, fall through the sample sweeping up smaller droplets, which have been nucleated at

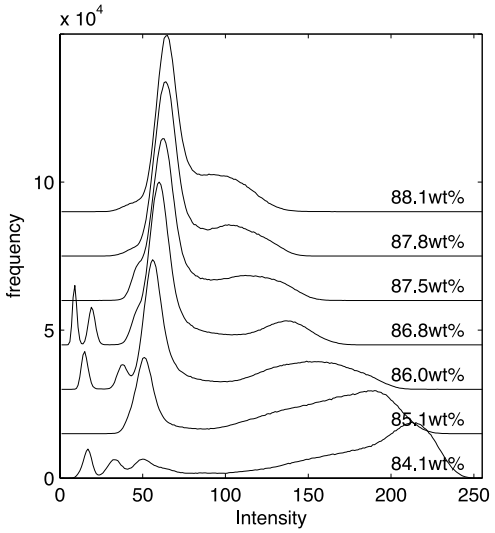

Fig. 4. Whole sample histograms for a dextran labeled sample as a function of time. (Peaks at intensities <50 correspond to slice which fall slightly above the upper surface of the sample.) Drying rate, $\Gamma = 7.42 \times 10^{-5}$ kg m^{-2} s^{-1}.

a slightly later time throughout the sample. The radii of the largest droplets in the sample are found to increase linearly with time, which can be explained using a simple model. Once the droplets reach the bottom of the sample they grow rapidly by coalescence and the arrival of further material from above. Mixtures with $\phi_{dex} = 0.5$ exhibited a bicontinuous morphology whose lengthscale varied with depth into the sample. This structure was found to 'drain' rapidly into a two layer structure of essentially pure phases.

Fig. 3 shows a sequence of images from near the bottom of a sample undergoing drying, in this case the dextran is fluorescently labelled. The images show changes in contrast between the dextran rich and dextran poor phases, which are the result of changes in composition. Notice also that evidence of secondary phase separation is apparent in the dextran rich droplets, as the system is quenched the droplets which originally formed close to the coexistence composition find that they contain excess PEG as the quench deepens and so undergo further phase separation. This is manifested as droplets of PEG rich material within larger droplets of dextran rich material.

More quantitative analysis of these images is possible. First, we are able to measure the overall water content of the drying film from its thickness, since we know the initial composition of the film—we assume that only water can leave the film and that the volumes of the components are simply additive. We find that the reduction of film thickness is linear with time so we can define a simple drying rate, Γ. This linear loss of water leads to an overall polymer content which increases ever more rapidly with time.

In our previous work we found that in the absence of other factors the evaporative loss of water from the surface would lead to a small depletion of water from the surface and that we might expect that the polymer concentration to

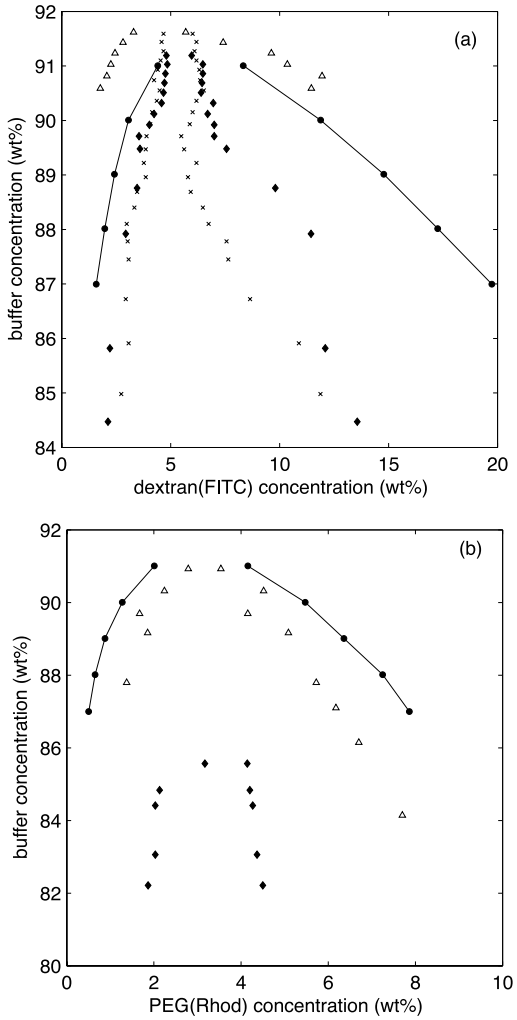

Fig. 5. (a) Dextran concentrations measured in phase separating systems at different drying rates (◆) 6.55×10^{-5} kg m^{-2} s^{-1}, (×) 7.42×10^{-5} kg m^{-2} s^{-1}, (△) 8.68×10^{-5} kg m^{-2} s^{-1} and (b) PEG concentrations measured in phase separating systems at different drying rates (◆) 6.29×10^{-5} kg m^{-2} s^{-1}, (△) 9.05×10^{-5} kg m^{-2} s^{-1}. Equilibrium phase compositions indicated by solid line.

be a little higher than the overall concentration by 1 wt% at most.

The second piece of compositional analysis is on the concentration of the labelled polymers in different phases. Fig. 4 shows image histograms for a sequence of images taken as a sample dried. These histograms plot the number of pixels having a particular intensity against the intensity. The two main peaks in the histogram correspond to the two phases, the peak area indicates the total area covered by a phase and the peak position is related to the concentration of the labelled species in that phase. The histogram can either be calculated over the whole sample or individual slices.

For this work peak maxima were identified manually and converted to composition using the calibration curves determined for single component mixtures. The results of this analysis are shown in Fig. 5(a) and (b) along with

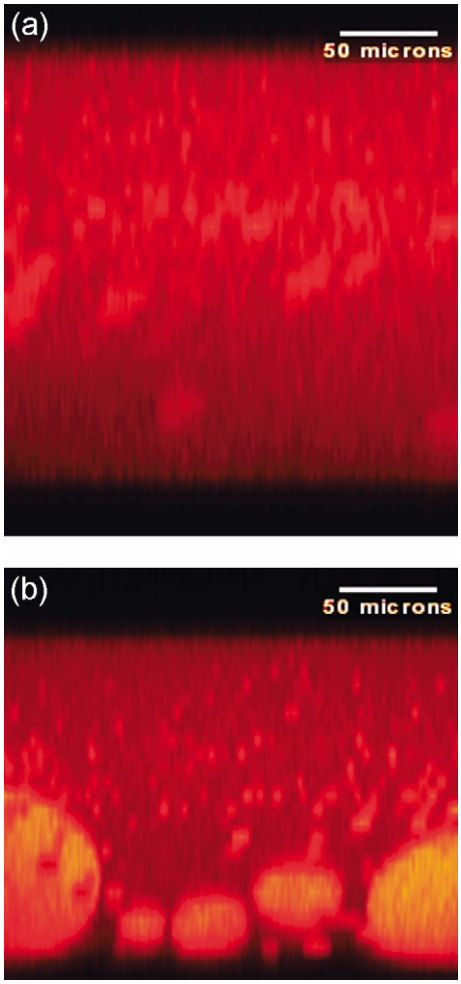

Fig. 6. Vertical slices through dextran labeled ternary solution drying at 7.42×10^{-5} kg m^{-2} s^{-1}, overall buffer contents of (a) 90.15 wt% and (b) 86.72 wt%.

measurements for the equilibrium composition. We note that this composition information does not correspond to a true phase diagram since equilibrium is not achieved.

This procedure is robust, similar results are obtained if the histograms are taken from the whole sample or just single slices and although there is some correlation between measured intensity and droplet sizes (bigger droplets tend to appear brighter) the effect of excluding smaller droplets from intensity calculations is small.

At lower drying rates we find an extended period during which droplets are observed but their compositions remain constant in time at a value far from the equilibrium composition, only at later times do the phase compositions start to change. This process is linked to the formation and descent of droplets. During the early stage of phase separation droplets of dextran rich material form and then fall through the sample. It is only when these droplets reach the bottom of the sample and start to grow rapidly by coalescence with subsequent arrivals that the phase compositions start to move towards the equilibrium values. This morphology is shown in Fig. 6.

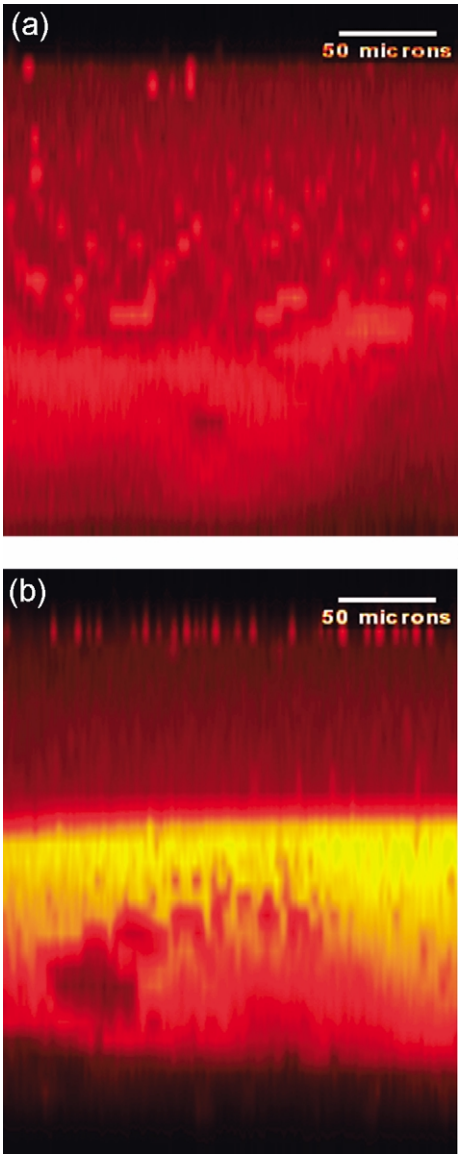

Fig. 7. Vertical slices through dextran labeled ternary solutions drying at 8.68×10^{-5} kg m^{-2} s^{-1}, overall buffer contents of (a) 91.62 wt% and (b) 91.03 wt%.

At high drying rates, phase compositions are close to the equilibrium compositions at all times. In these samples we observe gross phase separation into two layers from the earliest times, this is shown in Fig. 7.

We can see the effect of drying rate on phase separation by examining the overall water concentration at which the phase compositions start to move towards the equilibrium values as a function of drying rate. This data is shown in Fig. 8, and it shows that the threshold concentration increases towards the equilibrium composition as the drying rate is increased, although the trend is noisy.

These results are somewhat counterintuitive; one might expect that a system quenched more slowly would have compositions closer to the equilibrium compositions because more time is available for this equilibration to occur. However, in this system, it would appear that changes

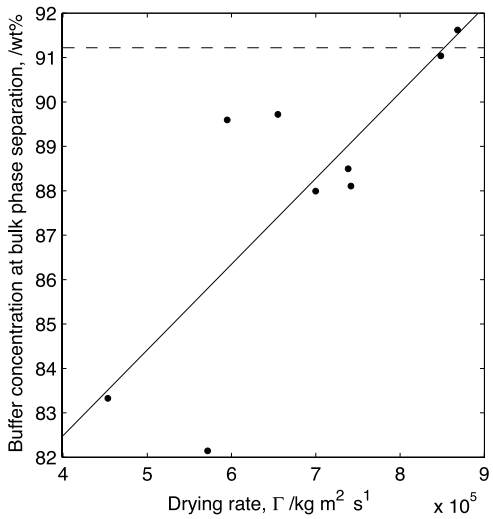

Fig. 8. Buffer concentration at which phase separation is observed throughout the sample as a function of drying rate for dextran labeled solutions. Solid line is a linear regression ($R^2 = 0.63$), broken line indicates the location of the equilibrium cloud point curve.

in the way the morphology develops play a dominant role in the way the phase compositions change. This is perhaps unsurprising since both the growth in physical dimensions of the phases and the change in composition are related to the movement of material around the system and so, naturally, they are linked.

4. Conclusions

We have shown that UV–visible spectroscopy and confocal microscopy can be used to measure phase compositions in a fluorescently labelled ternary polymer solution containing dextran, polyethylene glycol and water. Spectroscopic measurements on the equilibrium system show a phase diagram in agreement with data from unlabelled systems studied in the literature. A discrepancy between the coexistence curve and the cloud point curve can be explained by the polydispersity of the component polymers. We have carried out a simple calculation to confirm this, using the methods described by Solc.

Confocal microscopy was used to measure phase compositions in drying films. The development of observed phase compositions depends on the drying rate; at lower drying rates the phase compositions only start to move towards the equilibrium values when droplets of phase separated material reach the bottom of the sample and start to coalesce and grow rapidly. At higher drying rates, the phase compositions are relatively close to the equilibrium value, this change in behaviour is linked to a change in the developing morphology; at high drying rates gross phase separation into two layers is observed to occur very rapidly.

A drawback of this study was the inability to measure the compositions of both polymers simultaneously. This is not the result of a fundamental physical restriction on the method presented, but simply reflects the choice of fluorescent dyes used in this study. If a pair of dyes, which did not exhibit significant RET, were used then this restriction could be overcome. Such a system would also allow the indirect mapping of water concentration throughout the sample.

A further extension would be to label particular molecular weight components, this would make it possible to track in real time the distribution of the component. The kinetics of phase separation in polydisperse systems is of increasing theoretical interest [46–48] and such experiments could be important in aiding the development of kinetic models.

Acknowledgements

We would like to thank Brad Thiel for his many helpful suggestions and we are grateful to Unilever plc and EPSRC for funding this work.

References

[1] Aartsen JJv, Smolders CA. Eur Polym J 1970;6:1105–12.
[2] Hashimoto T, Kumaki J, Kawai H. Macromolecules 1983;16:641–8.
[3] Snyder HL, Meakin P, Reich S. J Chem Phys 1983;78:3334–6.
[4] Cumming A, Wiltzius P, Bates FS, Rosedale JH. Phys Rev A 1992;45:885–97.
[5] Ribbe AE, Hayashi M, Weber M, Hashimoto T. Polymer 1998;39:7149–51.
[6] Ribbe AE, Hashimoto T. Macromolecules 1997;30:3999–4009.
[7] Jinnai H, Koga T, Nishikawa Y, Hashimoto T, Hyde ST. Phys Rev Lett 1997;78:2248–51.
[8] Jinnai H, Nishikawa Y, Morimoto H, Koga T, Hashimoto T. Langmuir 2000;16:4380–93.
[9] Jinnai H, Yoshida H, Kimishima K, Funaki Y, Hirokawa Y, Ribbe AE, Hashimoto T. Macromolecules 2001;34:5186–91.
[10] Takeno H, Iwata M, Takenaka M, Hashimoto T. Macromolecules 2000;33:9657–65.
[11] Cahn JW. J Chem Phys 1957;28:258–67.
[12] Cahn JW. Acta Metall 1961;9:795–801.
[13] Cahn JW. J Chem Phys 1965;42:93–9.
[14] Binder K, Stauffer D. Phys Rev Lett 1974;33:1006–9.
[15] Lifshitz IM, Slyozov VV. Phys Chem Solids 1961;19:35–50.
[16] Siggia ED. Phys Rev A 1979;20:595–605.
[17] Hopkinson I, Myatt M. Macromolecules 2002;35:5153–60.
[18] Maeda Y, Yamamoto H, Ikeda I. Macromolecules 2003;36:5055–7.
[19] Wilson T. (Ed) Confocal microscopy. London: Academic Press; 1990.
[20] Chestnut MH. Curr Opin Colloid Interface Sci 1997;2:158–61.
[21] Ribbe AE. Trends Polym Sci 1997;5:333–7.
[22] Blaaderen Av, Wiltzius P. Science 1995;270:1177–9.
[23] Kegel WK, Blaaderen Av. Science 2000;287:290–3.
[24] Gasser U, Weeks ER, Schofield A, Pusey PN, Weitz DA. Science 2001;292:258–62.
[25] Weeks ER, Crocker JC, Levitt AC, Schofield A, Weitz DA. Science 2000;287:627–31.
[26] Kumacheva E, Li L, Winnik MA, Shinozaki DM, Cheng PC. Langmuir 1997;13:2483–9.
[27] Mitov Z, Kumacheva E. Phys Rev Lett 1998;81:3427–30.

[28] Serrano B, Baselga J, Bravo J, Mikes F, Sese L, Esteban I, Pierola IF. J Fluoresc 2000;10:135–9.
[29] Müller-Buschbaum P, Gutmann JS, Wolkenhauer M, Kraus J, Stamm M, Smilgies D, Petry W. Macromolecules 2001;34:1369–75.
[30] Diamond AD, Hsu JT. Biotechnol Tech 1989;3:119–24.
[31] Furuya T, Iwai Y, Tanaka Y, Uchida H, Yamada S, Arai Y. Fluid Phase Equilib 1995;103:119–41.
[32] Johansson G, Joelsson M. Polymer 1992;33:152–5.
[33] Grossman C, Tintinger R, Zhu J, Maurer G. Fluid Phase Equilib 1995; 106:111–38.
[34] Hasse H, Kany H-P, Tintinger R, Maurer G. Macromolecules 1995; 28:3540–52.
[35] Kany HP, Hasse H, Maurer G. J Chem Engng Data 1999;44:230–42.
[36] Kang C-H, Lee C-K, Sandler SI. Ind Engng Chem Res 1989;28: 1537–42.
[37] Sigma, Product Information Sheet; 1995.
[38] Myatt MJ. PhD Thesis. Department of Physics, University of Cambridge; 2002.
[39] Sjöback R, Nygren J, Kubista M. Spectrochim Acta A 1995;51: L7–L21.
[40] Lakowicz RL. Principles of fluorescence spectroscopy, 2nd ed. Dordrecht/New York: Kluwer Academic/Plenum Press; 1999.
[41] Koningsveld R, Staverman AJ. Kolloid-zeitschrift und Zeitschrift fur polymere 1967;218:114–24.
[42] Koningsveld R, Staverman AJ. J Polym Sci A2 1968;6:325–47.
[43] Sollich P. J Phys: Condens Matter 2002;14:R79–R117.
[44] Solc K, Koningsveld R. Collect Czech Chem Commun 1995;60: 1689–718.
[45] Kim MW. Colloids Surf, A 1997;18:145–54.
[46] Pagonabarraga I, Cates ME. Macromolecules 2003;36:934–49.
[47] Clarke N. Eur Phys J E 2001;4:327–36.
[48] Warren PB. Phys Rev Lett 1998;80:1369–72.